Electrical Engineering
https://doi.org/10.1007/s00202-021-01441-z

ORIGINAL PAPER

Cascaded H-bridge multilevel inverters optimization using adaptive grey wolf optimizer with local search

Oğuzhan Ceylan[1,2] · Mehdi Neshat[3] · Seyedali Mirjalili[3,4]

Received: 23 July 2021 / Accepted: 28 October 2021

Abstract
With the transformation of transmission and distribution grids into smart grids that are more dominated by renewable energy, power electronics-based inverters that can improve power quality are becoming more visible. In order to maximize the output voltage quality and reduce the total harmonic distortion (THD), efficient operation of inverters is required. Therefore, in this paper, the problem of harmonic elimination in multilevel inverters is solved by using an adaptive grey wolf optimizer with local search. We have performed a grid search-based landscape analysis of the seven-level inverter to understand the behaviour of the proposed algorithm. For verification, the numerical results of the proposed adaptive grey wolf optimizer are compared with those of the original grey wolf optimization algorithm, a modified version of the grey wolf optimization algorithm, the particle swarm optimization algorithm, multi-verse optimization algorithm, and salp swarm algorithm. In the simulations, we solved the optimization model for three different structures of multilevel inverters (7, 11, and 15 levels) by changing the modulation indexes. It is found that the adaptive grey wolf optimization provides lower total harmonic distortion for different modulation indexes.

Keywords Adaptive grey wolf optimizer · Harmonic distortion · Local search · Multilevel inverters · Selective harmonic elimination · Optimization · Algorithm

1 Introduction

For environmental and economic reasons, renewable energy sources are increasingly being integrated into electrical power systems. However, wind turbines (WTs) and photovoltaics (PVs) cause fluctuations in power output and voltage levels in distribution systems. Therefore, more control actions are required. In addition to classical control devices, power system operators can also use inverters for fast, efficient control operations, as these can also help to reduce switching losses and maintain a more balanced voltage profile of the distribution system [1].

Multilevel inverters (MLIs) can be classified as diode-clamped, flying capacitor, and cascaded H-bridge inverters depending on the topology [2]. MLIs consist of multiple circuit components such as DC power sources, semiconductors, switches, which mainly generate an AC voltage. The applications of multilevel inverters are not limited to PV and WT systems. Paper [3] gives a comprehensive overview of MLI techniques suitable for electric vehicles. Another application area is UPS applications [4]. A recent study proposes a new design of an MLI for induction motor drive control that can be used for water pumping in marine applications [5]. Mainly, the classical topologies are used for most applications, but in recent years, there are attempts to develop other topologies, an overview of these can be found in [6,7].

The optimal determination of the switching angle of MLIs helps to minimize the total harmonic distortion (THD). The approaches to solve this kind of problem can be divided into two: analytical and numerical methods. As for the numeri-

✉ Oğuzhan Ceylan
oguzhan.ceylan@marmara.edu.tr

Mehdi Neshat
mehdi.neshat@laureate.edu.au; neshat.mehdi@gmail.com

Seyedali Mirjalili
ali.mirjalili@torrens.edu.au

[1] Management Information Systems Department, Kadir Has University, Istanbul, Turkey

[2] Electrical and Electronics Engineering Department, Marmara University, Istanbul, Turkey

[3] Center for Artificial Intelligence, Research and Optimization, Torrens University Australia, Brisbane, QLD 4006, Australia

[4] Yonsei Frontier Lab, Yonsei University, Seoul, South Korea

Published online: 19 November 2021

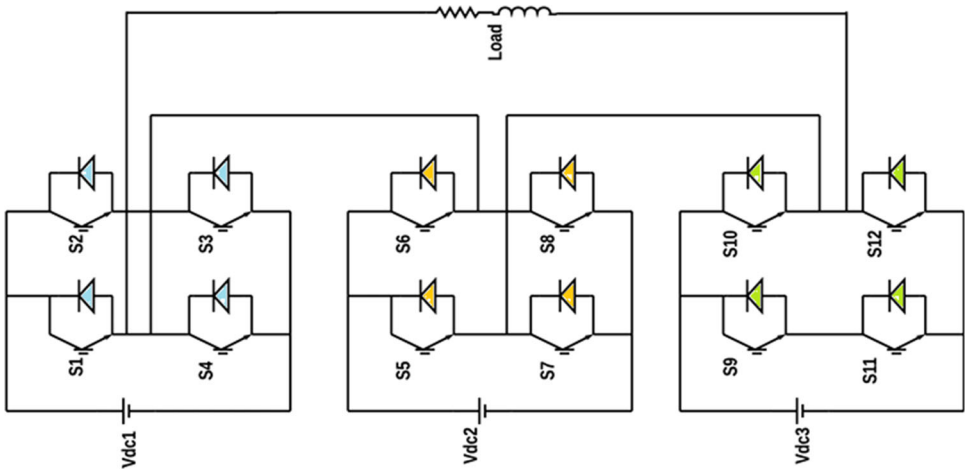

Fig. 1 Single-phase, 7-level MLI from [27]

cal method, Newton–Raphson has been used both for solving the selective harmonics equations (SHE) for MLIs [8] and for solving SHE of a relatively recent design of a flying capacitor MLI [9]. In [10], the authors combine artificial neural networks (ANN) with the Newton–Raphson method: The optimal switching angles are used to train the ANN, then the results are used as initial estimates for the NR-based optimization method. Some other derivative based numerical approaches used to solve the SHE problem are gradient optimization [11] and sequential quadratic programming [12] methods. Derivative-free methods have also been used to solve the harmonic elimination problem. One of the first attempts was based on genetic algorithms (GA) [13]. Later, other heuristics such as particle swarm optimization (PSO) [14], differential evolution [15] harmony search algorithm [16,17] were implemented. More details on the implemented approaches for MLIs can be found in [18]. In addition, see [19] for applications of meta-heuristic methods to the converter problem. A recent work solves the SHE problem using a hybridized PSO and GA method [20]. The authors of [21], use the whale optimization algorithm developed by Mirjalili and Lewis (WOA) based on the behaviour of whales [22]. The moth flame optimization (MFO) algorithm [23] was used in [24] to solve the problem of harmonic elimination of MLIs. Two recently developed heuristic algorithms, namely the multiverse optimization algorithm (MVO) [25] and the salp swarm optimization algorithm (SSA) [26], were also used in [27].

This paper improves on recent attempts to solve MLI optimization problems presented in [24] and [27], and more specifically,

- Solves an optimization model that aims to eliminate harmonics and THD.
- Utilizes an adaptive GWO (AGWO) [28], which consists of a chaotic map for the control parameter (α) and an adaptive reset mechanism with local search. The performance of AGWO is compared with a modified GWO [29], standard GWO, PSO, MVO and SSA to solve the optimization model.
- Compares the simulation results of 7-, 11- and 15-level MLIs with different modulation indexes in terms of numerical accuracy.

The organization of the paper is given as follows. The next section gives the optimization model used to minimize THD and harmonics. In Sect. 3, we give a detailed landscape analysis for MLIs. Section 4 explains the standard GWO, and details the modifications implemented for AGWO. Before conclusion, in Sect. 5, we give the numerical simulation results.

2 Optimization model for cascaded H-bridge multilevel inverters

We show the circuit diagram of a 7-level MLI with equal DC sources connected to a single-phase H-bridge inverter in Fig. 1.

Note that the number of output voltage levels is $2 \times k + 1$, where k is the number of individual DC sources. The Fourier transform of a stepped waveform with s steps is given as: [30]:

$$V(\omega t) = \frac{4V_{\text{dc}}}{\pi} \sum_{n} [\cos(n\theta_1) + \cos(n\theta_2) + \cdots + \cos(n\theta_s)] \times \sin\left(\frac{n\omega t}{n}\right), n = 1, 3, 5, 7, \ldots \quad (1)$$

where ω, V_{dc} and θ_i show the angular velocity, DC source's voltage magnitude, and conducting angle of step i, respectively. One can determine the coefficients in Eq. (1) using [30]:

$$H(n) = \frac{4}{n\pi}\sum_{n}[\cos(n\theta_1) + \cos(n\theta_2) + \cdots + \cos(n\theta_s)] \quad n = 1, 3, 5, 7, \ldots \tag{2}$$

The switching angles $\theta_1, \theta_2, \ldots, \theta_n$ must satisfy:

$$\theta_1 \leq \theta_2 \leq \cdots \leq \theta_n \leq \frac{\pi}{2} \tag{3}$$

Total harmonic distortion (THD) can be mathematically shown as:

$$THD = \frac{\sqrt{(\sum_{n=3,5,7\ldots}^{n=49} V_n^2)}}{V_1^2} \tag{4}$$

Conventionally, optimization models aim to minimize the odd lower order harmonics. This approach can be briefly summarized as follows. The number of harmonics that can be eliminated is smaller than the number of H-Bridges (HB).

One can eliminate at most $n-1$ lower-order harmonics if a MLI with n HBs is considered, for 3 HBs, this can achieved by solving following equations [24]:

$$\begin{aligned} F(n) &= \cos(\theta_1) + \cos(\theta_2) + \cos(\theta_3) - 3m_1 \\ F(5n) &= \cos(5\theta_1) + \cos(5\theta_2) + \cos(5\theta_3) \\ F(7n) &= \cos(7\theta_1) + \cos(7\theta_2) + \cos(7\theta_3) \end{aligned} \tag{5}$$

Similarly, for an 11 level inverter, with 5 HBs, and for a 15-level inverter with 7 HBs, the required number of equations to be solved are 4 and 6, respectively, and can be represented mathematically as follows:

$$\begin{aligned} F(n) &= \cos(\theta_1) + \cos(\theta_2) + \cos(\theta_3) + \cos(\theta_4) + \cos(\theta_5) - 5m_1 \\ F(5n) &= \cos(5\theta_1) + \cos(5\theta_2) + \cos(5\theta_3) + \cos(5\theta_4) + \cos(5\theta_5) \\ F(7n) &= \cos(7\theta_1) + \cos(7\theta_2) + \cos(7\theta_3) + \cos(7\theta_4) + \cos(7\theta_5) \\ F(11n) &= \cos(11\theta_1) + \cos(11\theta_2) + \cos(11\theta_3) + \cos(11\theta_4) + \cos(11\theta_5) \\ F(13n) &= \cos(13\theta_1) + \cos(13\theta_2) + \cos(13\theta_3) + \cos(13\theta_4) + \cos(13\theta_5) \end{aligned} \tag{6}$$

$$\begin{aligned} F(n) &= \cos(\theta_1) + \cos(\theta_2) + \cos(\theta_3) + \cos(\theta_4) + \cos(\theta_5) + \cos(\theta_6) + \cos(\theta_7) - 7m_1 \\ F(5n) &= \cos(5\theta_1) + \cos(5\theta_2) + \cdots + \cos(5\theta_6) + \cos(5\theta_7) \\ F(7n) &= \cos(7\theta_1) + \cos(7\theta_2) + \cdots + \cos(7\theta_6) + \cos(7\theta_7) \\ F(11n) &= \cos(11\theta_1) + \cos(11\theta_2) + \cdots + \cos(11\theta_6) + \cos(11\theta_7) \\ F(13n) &= \cos(13\theta_1) + \cos(13\theta_2) + \cdots + \cos(13\theta_6) + \cos(13\theta_7) \\ F(17n) &= \cos(17\theta_1) + \cos(17\theta_2) + \cdots + \cos(17\theta_6) + \cos(17\theta_7) \\ F(19n) &= \cos(19\theta_1) + \cos(19\theta_2) + \cdots + \cos(19\theta_6) + \cos(19\theta_7) \end{aligned} \tag{7}$$

In (5), (6), and (7), m_1 represents the modulation index, which is the division of the amplitude command of the inverter for a sine wave output phase voltage to the maximum attainable amplitude of the inverter [30].

In this study, we use the same model as of [27] aiming to minimize the objective function given as:

$$\begin{aligned} &\text{minimize} \sqrt{\frac{\sum_{n=3,5,7\ldots}^{n=49} V_n^2}{V_1}} + |\cos(\theta_1) + \cos(\theta_2) + \cdots + \cos(\theta_k) - km| \\ &\text{subject to} \quad \theta_1 \leq \theta_2 \leq \cdots \theta_k \leq 90^\circ \end{aligned} \tag{8}$$

where k is 3, 5, and 7 for 7, 11, and 15 level MLIs in Eq. 8, respectively.

3 Landscape analysis of cascaded H-bridge multilevel inverters

One of the most popular methods to understand the behaviour of complex optimization problems is the landscape analysis algorithm [31]. In this process, various characteristics of the problems are considered by evaluating the landscape features. One of the main goals is to classify the problems into distinct classes with regard to these features.

Landscape analysis methods are applied to a wide range of complex and real-world optimization problems, which can be classified into three groups: (1) real-world engineering problems, (2) recently, machine learning applications have also been considered, (3) mathematical and stochastic benchmarks of classical optimization problems. In order to provide a systematic mechanism for exploring and interpreting the behaviour of meta-heuristics, landscape analysis techniques are also recommended.

In this paper, we perform a simple and effective method for landscape analysis called grid search. In this algorithm, a

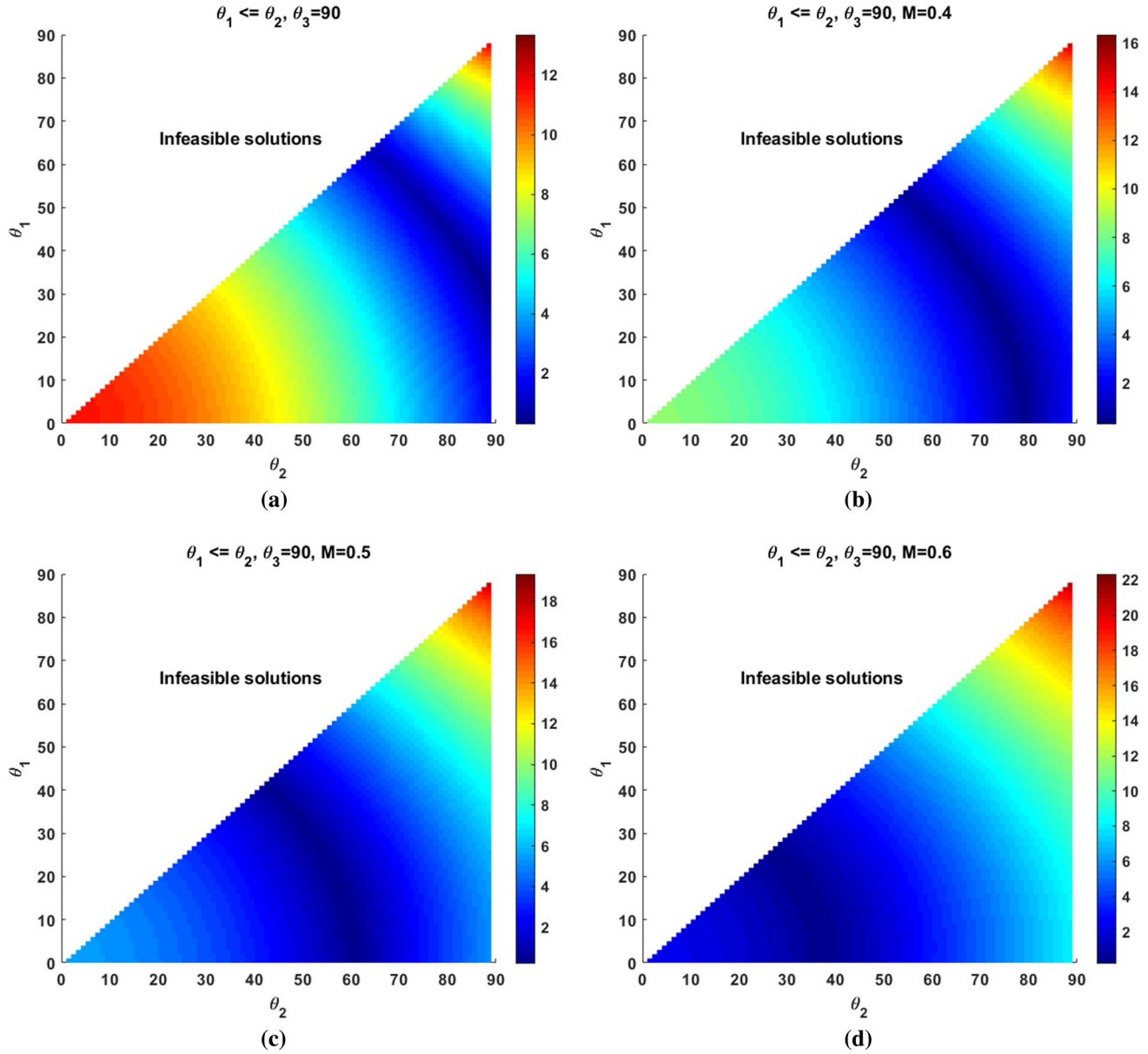

Fig. 2 Landscape analysis of the 7-level cascade MLI with different ranges of M when $\theta_1 \leq \theta_2$, and $\theta_3 = 90°$, **a** $M = 0.3$, **b** $M = 0.4$, **c** $M = 0.5$ and **d** $M = 0.6$

regular and symmetric sampling process is iterated to observe different aspects of the search space of the cascaded H-bridge multilevel inverter problem. The target of this analysis is the 7-level inverter problem considering the primary constraint $\theta_1 \leq \theta_2 \leq \theta_3$. We assume that $\theta_3 = 90°$ remains fixed during the landscape analysis, and the main focus is on observing the behaviour of angles θ_1 and θ_2. An extensive sampling of all possible configurations of the two inverter angles θ_1 and θ_2 is performed, assuming the range of M from 0.3 to 1.0.

The results of the landscape analysis are interesting and show considerable detail of the search space for the problem applied. In Fig. 2, the main observation is that the best found configurations of angles vary depending on the value of the modulation index M. Interestingly, increasing the modulation index leads to a shift of the optimal settings (area) to small values of both $\theta 1$ and θ_2. For example, when M is 0.3, the best angles found are $80° \leq \theta_2 \leq 90°$ and $\theta_1 \leq 70$; however, increasing the modulation index to 0.6 leads to a different search space and the effective solutions are in the range of $\theta_1, \theta_2 \leq 50$.

In the remainder of this landscape analysis, we develop and evaluate the performance of fitness values for a modulation index greater than 0.6. The experimental results of the landscape analysis can be seen in Fig. 3. For this range of M,

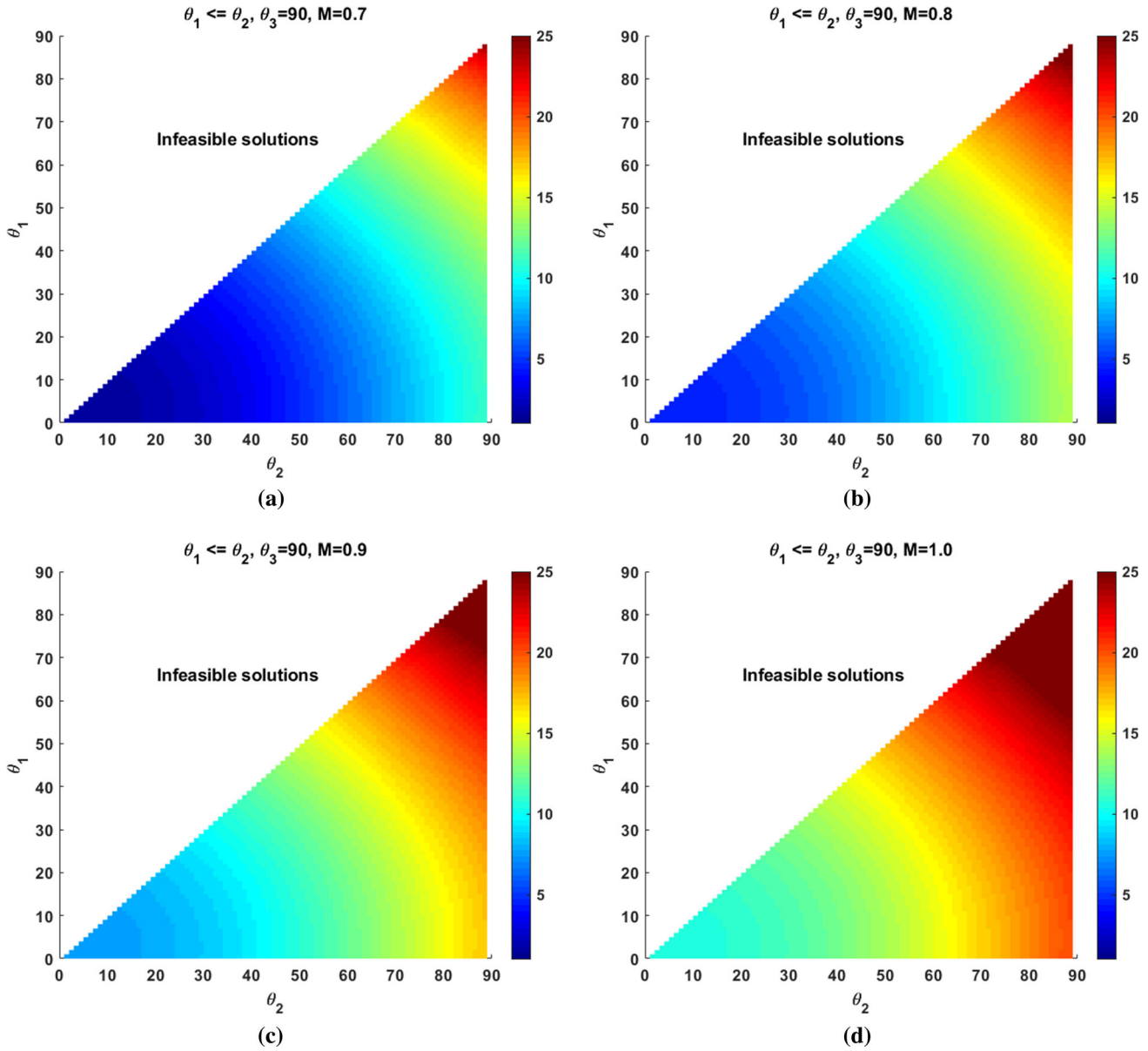

Fig. 3 Landscape analysis of the 7-level cascade MLI with different ranges of M when $\theta_1 \leq \theta_2$, and $\theta_3 = 90°$, **a** $M = 0.7$, **b** $M = 0.8$, **c** $M = 0.9$ and **d** $M = 1.0$

we can see that when the value of θ_3 is equal to 90° and does not change during the assessment, the best found areas shift to smaller angles of both θ_1 and θ_2.

4 Meta-heuristic algorithms

In this section, we first introduce the grey wolf optimizer and its variants. Then, its performance is improved using an adaptive mechanism and local search.

4.1 Grey wolf optimizer (GWO)

The Grey wolf optimizer (GWO) algorithm[32] is described as a bio-inspired and population-based stochastic approach that mimics some social behaviours of grey wolves in a pack. In a wolf pack, there are four types of roles: The alpha wolf is responsible for managing the others, beta and delta wolves are responsible for helping the alpha in managing, and other members (called omegas) participate in exploring the search space. Mainly, GWO simulates the hunting process by searching the prey, encircling, chasing, hunting and attacking prey. Indeed,GWO mimics the characteristics

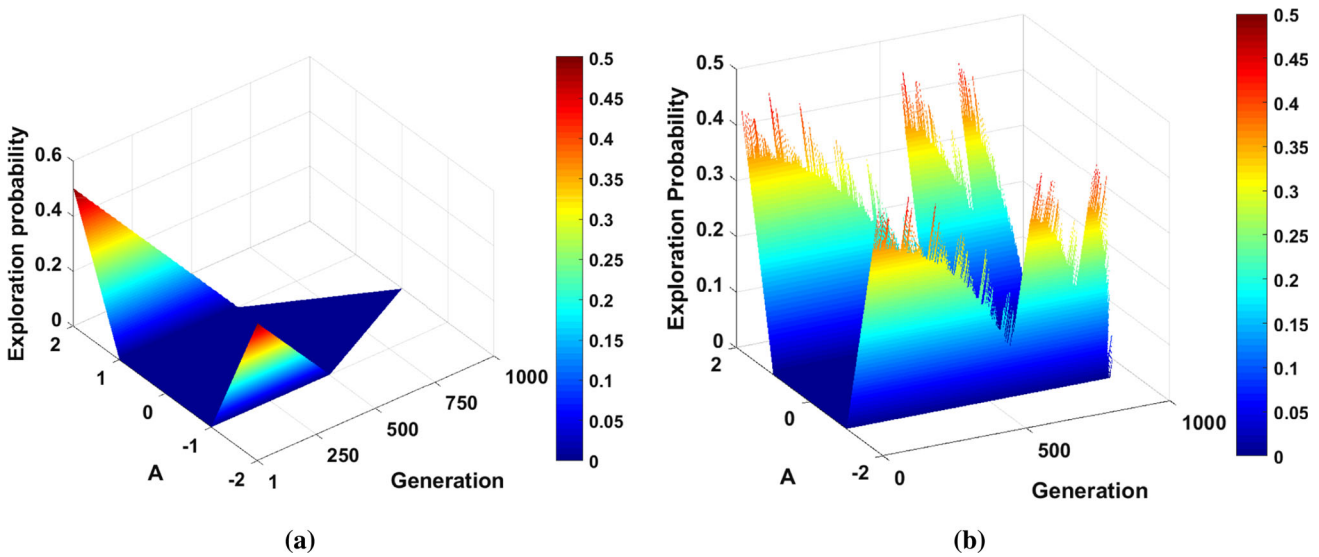

Fig. 4 **a** The probability exploration of GWO per each generation. **b** AGWO's adaptation mechanism example for the control vector (a) in AGWO (from [28])

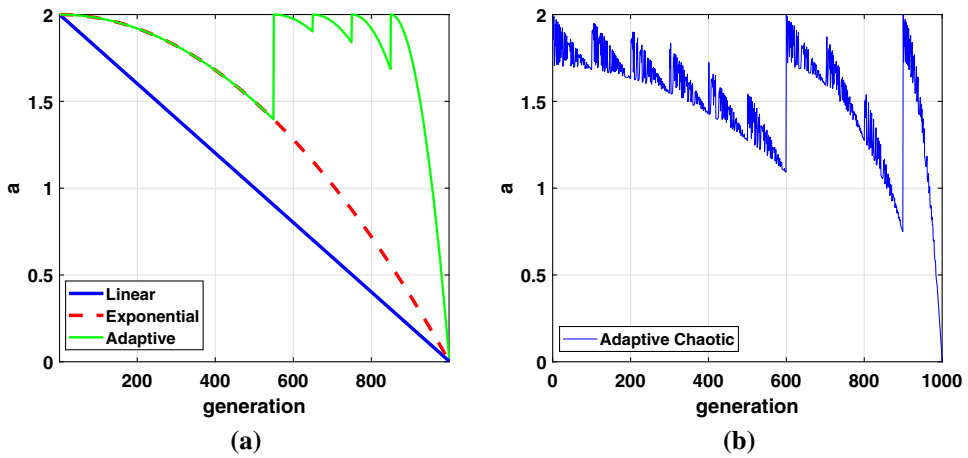

Fig. 5 **a** the main method of control variable a decreased linearly [32] (blue line), polynomially shrunken (red line) [29], and can be adaptive (green line) proposed in this paper. **b** Shows decay plot that consolidate both adaptive and chaotic decay

of the hunting process as follows: (1) exploring for the prey (optimum), (2) encircling and enclosing the prey, (3) hunting and finally attacking the targets.

4.1.1 Encircling step

$$\mathbf{D} = |\mathbf{C}.\mathbf{X_p}(t) - \mathbf{X}(t)| \tag{9}$$

$$\mathbf{X}(t+1) = \mathbf{X_p}(t) - \mathbf{A}.\mathbf{D} \tag{10}$$

where $\mathbf{D}$ depicts the distance between the prey location $\mathbf{X_p}$ with another member $\mathbf{X}$ in the prevailing repetition (t). Furthermore, the vectors $\mathbf{A}$ and$\mathbf{C}$ play an important role, having a strong influence for adjusting the exploration and exploitation behaviours and are computed by Eqs. 11 and 13:

$$\mathbf{A} = 2.\mathbf{a}.\mathbf{r_1} - \mathbf{a} \rightarrow 0 \leq a \leq 2 \tag{11}$$

$$a = 2 - \text{iter}.\left(\frac{2}{\text{Max}_{\text{iter}}}\right) \tag{12}$$

$$\mathbf{C} = 2.\mathbf{r_2} \tag{13}$$

where a is reduced linearly from 2 to 0 through the optimization means. r_1 and r_2 are two random numbers between 0 and 1.

4.1.2 Hunting

In order to obtain a thriving exploration of the search area, the values of candidates should be changed with regard to the knowledge received from three best-found candidates (alpha,

beta and delta). The main reason for this is that GWO considers a prior that a nearby optimum can be observed among this triangle area. To update the position of solutions, the following formulas (Eqs. 14, 15 and 16) are introduced.

$$\mathbf{X}(t+1) = \frac{\mathbf{X_1} + \mathbf{X_2} + \mathbf{X_3}}{3} \tag{14}$$

$$\begin{aligned} &\mathbf{X_1} = \mathbf{X}_\alpha(t) - \mathbf{A_1} \cdot \mathbf{D}_\alpha, \mathbf{X_2} = \mathbf{X}_\beta(t) - \mathbf{A_2} \cdot \mathbf{D}_\beta \\ &\mathbf{X_3} = \mathbf{X}_\delta(t) - \mathbf{A_3} \cdot \mathbf{D}_\delta \end{aligned} \tag{15}$$

$$\begin{aligned} &\mathbf{D}_\alpha = |\mathbf{C_1} \cdot \mathbf{X}_\alpha - \mathbf{X}|, \mathbf{D}_\beta = |\mathbf{C_2} \cdot \mathbf{X}_\beta - \mathbf{X}| \\ &\mathbf{D}_\delta = |\mathbf{C_3} \cdot \mathbf{X}_\delta - \mathbf{X}| \end{aligned} \tag{16}$$

4.1.3 Attacking the prey (exploitation)

The last behaviour formulated is hunting, which involves attacking prey and focusing on optimal situations. Attacking can be done by decreasing a from 2 to 0. In Fig. 5 one can see several possible approaches. This can be achieved mathematically by decreasing the variable a from 2 to 0 on a regular basis. It can be observed that when $|\mathbf{A}| < 1$ candidates focus on attacking the prey. This process evolves like a local search (exploitation process). On the other hand, $|\mathbf{A}| > 1$ drives to a global exploration (diversification).

4.2 Modified grey wolf optimizer (mGWO) [29]

In the standard GWO, 50% of the repetitions are dedicated to exploration and the other half to exploitation, achieving a great balance between the two main search processes. However, for some specific problems, we may find that this static mechanism cannot be effective. To address this shortcoming, a modified GWO (mGWO) has been proposed[29]. mGWO mainly focuses on the appropriate balance between exploration and exploitation, which leads to an optimal representation of the optimization algorithm. Figure 5a represents the proposed exponential control parameter of a based on Eq. 17.

$$a = 2 - \text{iter}^2 \cdot \left(\frac{2}{\text{Max}_{\text{iter}}^2} \right) \tag{17}$$

Utilizing this exponential decay equation, the evaluation numbers which are used for both exploration and exploitation are divided into 70% and 30%, respectively.

4.3 Adaptive grey wolf optimizer (AGWO)

Since $\mathbf{A}$ is able to regulate both diversification ($|\mathbf{A}| > 1$) and intensification ($|\mathbf{A}| < 1$), it is one of the most important parameters of GWO. Equation 11 shows that the vector of $\mathbf{A}$ values lies between $-2a$ and $2a$ ($\mathbf{A} \in [-2a, 2a]$), where a decreases linearly from 2 to 0 during the optimization process. This means that the exploration probability ($|\mathbf{A}| > 1$) is 0.5 at the beginning of the iteration and then decreases linearly to 0 when the search process is in the middle. In contrast, the exploitation probability in the first iteration is 0.5, which is equal to the exploration probability (providing a balanced heuristic setting at the commencement); nevertheless, the exploitation probability is advanced to 1 when half of the repetitions are dedicated ($iter = \text{Max}_{\text{iter}}/2$). Notably, in the resting iterations ($\text{Max}_{\text{iter}}/2$),the exploitation probability is fixed at 1, even though the exploration probability is 0 without any conversion. This lack of settings could be one of the reasons for possible convergence problems GWO may encounter. Fig. 4a shows this unbalanced search performance. To solve this deficiency, several mechanisms have been proposed as follows.

Mittal et al. [29] introduced an enhanced version in order to update **a** in (mGWO), which decayed more gently to improve exploration. Figure 5a depicts this more gradual decay function. Nevertheless, in this static mechanism, after 70% of iterations, the value of a still declined under 1. The same adjustment was proposed by Long et al. [33] in their improved grey wolf optimizer (IGWO). More recently, Saxena et al. [34] balanced the decay function utilizing a β-chaotic sequence to provide for faster vibration between exploration and exploitation conditions through the parameter decay process.

Previous research has recommended a variety of approaches to improve the a parameter, and these approaches have not considered GWO performance during optimization. In this paper, we propose an adaptive strategy to update the a control variable of the GWO (AGWO). Here, the optimization achievement is taken into account, and after a predefined interval of ρ iterations in which the best found configuration fails to reach the alpha, the control parameter should be updated to 2 again. Moreover, a chaotic distribution is embedded in the mapping by a normalization function to achieve a reasonable balance between exploration and exploitation. The main contributions of AGWO are as follows:

1. Producing and mixing a chaotic sequence with the control parameter (a) in every repetition. In order to reach the best achievement, the best-performed chaotic map is used [28]. Equation 18 confers the applied chaotic maps in the adaptive approach ($\mu = 1.07$).

$$x_{i+1} = \mu(7.86x_i - 23.31x_i^2 + 28.75x_i^3 - 13.302875x_i^4) \tag{18}$$

2. The mathematical equation in order to apply the normalization function for distributing the chaotic order within the upper and lower bias can be expressed by Eq. 19.

Table 1 Experimental optimization results of adaptive GWO, mGWO, standard GWO, PSO, MVO, and SSA: switching angles, modulation, and THD for 7-level MLI

M	θ_1	θ_2	θ_3	THD%	θ_1	θ_2	θ_3	THD%
	AGWO				GWO			
0.3	26.170	89.855	90.000	27.664	26.237	90.000	90.000	28.347
0.4	18.911	75.286	90.000	26.271	17.749	73.025	90.000	28.954
0.5	13.109	57.826	90.000	18.481	14.748	56.134	90.000	19.714
0.6	11.128	37.162	88.741	15.711	12.012	37.657	90.000	15.925
0.7	9.605	35.126	72.688	15.383	8.192	35.525	70.038	15.651
0.8	8.975	30.050	56.806	11.003	9.475	30.590	55.537	11.040
0.9	5.317	21.432	39.230	13.558	6.391	23.793	38.407	13.962
1	5.939	15.902	24.112	23.900	0.792	9.941	27.110	25.733
	mGWO				PSO			
0.3	26.364	89.758	89.997	28.115	30.223	87.459	90.000	32.964
0.4	19.074	75.218	90.000	29.980	19.106	75.220	89.999	29.999
0.5	16.534	57.207	90.000	20.507	16.453	57.252	90.000	20.520
0.6	10.857	37.123	88.841	15.977	10.886	37.192	88.775	15.980
0.7	10.570	35.638	72.274	16.046	10.527	35.548	72.350	16.050
0.8	9.780	29.983	56.734	11.094	9.802	29.999	56.731	11.100
0.9	6.980	21.068	39.271	14.079	6.965	21.091	39.252	14.080
1	5.639	15.302	24.112	24.120	5.040	12.827	21.153	26.930
	MVO [27]				SSA [27]			
0.4	19.026	75.248	90.00	30.00	18.998	75.258	90.00	30.00
0.5	16.43	57.257	90.00	20.520	16.454	57.251	90.00	20.520
0.6	10.896	37.176	88.783	15.980	10.884	37.190	88.776	15.980
0.7	10.572	35.503	72.368	16.050	10.533	35.546	72.350	16.050
0.8	9.827	30.00	56.726	11.100	9.803	30.00	56.733	11.100
0.9	6.961	21.081	39.259	14.080	6.976	21.096	39.247	14.80
1	5.040	12.827	21.152	26.930	5.040	12.827	21.152	26.930

$$N_{m_{\text{iter}}} = \text{CN}_m^{\text{Max}} - \left(\frac{CN_m^{\text{Max}} - \text{CN}_m^{\text{Min}}}{\text{Max}_{\text{iter}_N}} \right) \times \text{iter}_N \quad (19)$$

where the upper and lower values of the normalization function are as follows: $CN_m^{\text{Max}} = 0.3$ and $CN_m^{\text{Min}} = 10^{-6}$, respectively. Both CN_m^{Max} and CN_m^{Min} handle the chaotic distribution of the employed chaotic map and engage the optimization method flips between the exploration and exploitation stages sequentially. $\text{Max}_{\text{iter}_N}$ is the maximum iterations in each period. Therefore, the normalized chaotic values (CC_{iter}) can be produced by Eq. 20:

$$CC_{\text{iter}} = N_{m_{\text{iter}}} * Cf \quad (20)$$

where Cf is produced by the proposed chaotic map. Fig. 4b and d shows an example of the adaptive chaotic mechanism. The chaotic sequence is mixed in the control vector **a** and is presented as follows:

$$a = (2 - CN_m^{\text{Max}}) - \left(\text{iter}_c^2 \times \frac{2 - CN_m^{\text{Max}}}{\text{Max}_{\text{iter}_c}^2} \right) + CC_{\text{iter}} \quad (21)$$

3. Proposing an adaptive strategy to update the control vector where the optimization outcomes are not acquired for ρ iterations. Where search stagnates in this process, the control vector will be reset at upper value, and then the decay inclination of the control vector is set to a sharper gradient. This occurs in a flip from exploitation ($|\mathbf{a}| < 1$) to exploration whenever search faced with the stagnation.

Figure 5 shows three different mechanisms to update the control vector such as linear and polynomial (a), and one example of the adaptive chaotic method in [28]. Consequently, the algorithm of AGWO can be seen in 1).

Table 2 Experimental optimization results of adaptive GWO, mGWO, standard GWO, PSO, MVO, and SSA: switching angles, modulation index, and THD for 11-level MLI

M	θ_1	θ_2	θ_3	θ_4	θ_5	THD%
	AGWO					
0.3	12.455	16.068	36.305	66.569	90.000	12.250
0.4	6.609	33.018	56.712	90.000	90.000	12.220
0.5	8.001	27.851	49.510	89.520	90.000	10.360
0.6	6.477	22.971	40.241	60.467	90.000	8.540
0.7	8.346	21.832	35.146	54.841	88.723	8.090
0.8	5.618	17.691	29.036	41.976	61.106	6.150
0.9	2.305	17.745	29.311	44.735	56.990	7.170
1	10.159	19.831	26.646	39.123	54.063	8.540
	GWO					
0.3	13.4581	41.4077	90.000	90.000	90.000	15.312
0.4	5.1283	34.5467	51.0171	90.000	90.000	13.268
0.5	8.7712	28.5109	50.2095	89.6664	90.000	10.394
0.6	4.7558	22.7719	41.3156	61.1441	90.000	9.071
0.7	5.9302	18.1382	35.0452	52.6352	90.000	8.331
0.8	5.8701	17.416	29.8623	43.2621	62.148	6.174
0.9	0.6145	10.8839	25.1946	35.0255	50.1267	10.227
1	14.6959	16.9728	17.5521	34.1317	60.5437	14.335
	mGWO					
0.3	6.985	27.562	63.436	90.000	90.000	13.450
0.4	13.083	33.860	53.630	90.000	90.000	12.660
0.5	9.150	27.858	51.045	89.752	90.000	10.400
0.6	9.279	23.704	40.066	59.360	90.000	8.800
0.7	6.262	18.394	37.135	53.748	90.000	8.220
0.8	6.368	17.435	29.015	41.534	61.595	6.220
0.9	0.021	15.457	22.710	36.966	53.323	9.300
1	1.239	7.781	28.201	37.809	39.432	11.000
	PSO					
0.3	15.958	53.269	90.000	90.000	90.000	18.534
0.4	10.772	36.271	77.792	89.999	89.999	17.080
0.5	9.232	28.010	51.360	89.712	89.963	10.400
0.6	7.435	22.937	42.107	69.783	89.999	10.080
0.7	6.614	19.892	33.508	50.169	84.722	8.720
0.8	5.581	17.251	29.755	43.353	69.972	6.190
0.9	4.190	12.440	22.227	30.869	42.087	12.640
1	1.814	4.789	8.450	11.428	15.274	40.550
	MVO [27]					
0.4	10.865	36.167	77.840	90.00	90.00	17.076
0.5	9.193	27.975	51.396	89.690	89.979	10.404
0.6	7.658	22.919	42.053	69.797	90.00	10.075
0.7	6.575	19.837	33.481	50.174	84.756	8.723
0.8	5.525	17.211	29.822	43.373	62.995	6.1860
0.9	4.288	12.802	21.822	31.007	42.074	12.640
1	1.814	4.791	8.449	11.426	15.268	33.550

Table 2 continued

M	θ_1	θ_2	θ_3	θ_4	θ_5	THD%
	SSA [27]					
0.4	10.884	36.143	77.850	90.00	90.00	17.076
0.5	9.267	28.196	51.221	89.740	89.950	10.405
0.6	7.508	22.934	42.078	69.794	90.00	10.073
0.7	6.602	19.849	33.469	50.215	84.724	8.722
0.8	5.591	17.264	29.734	43.354	62.977	6.185
0.9	4.316	12.679	21.978	30.972	42.051	12.639
1	1.814	4.789	8.450	11.428	15.274	33.546

Algorithm 1 *Adaptive Grey Wolf optimizer (AGWO)*

procedure AGWO
  $d = len(\langle\theta_1^1, \theta_2^1, ..., \theta_d^1\rangle) \Rightarrow \theta_1 \leq \theta_2 \leq ... \leq \theta_d, 0 \leq \theta_i \leq \frac{\pi}{2}$
  $N = 30, M = 5$ ▷ Population size and performance index
  $\mathbb{S} = \{\langle\theta_1^1, \theta_2^1, ..., \theta_d^1\rangle, \ldots, \langle\theta_1^N, \theta_2^N, ..., \theta_d^N\rangle\}$
  Initialise parameters $a, A, C, CN_m^{Max}, CN_m^{Min}, \rho, Max_{iter_N}$
  X=*The best solution from* $\langle S_1, \ldots, S_N\rangle$ ▷ *Find three best*
  X_{fi}=The second best solution from $\langle S_1, \ldots, S_{N-1}\rangle$
  X=The third best solution from $\langle S_1, \ldots, S_{N-2}\rangle$
  while stillTime() ***do***
    for *i in* $[1, .., N]$ ***do***
      Update S_i
      if S_i *is not feasible* **then**
        $f(S_i) = \sum_{i=I}^{d} violation_i * PF + f(S_i))$
      end if
    end for
    $THD = Eval([S_1, S_2, \ldots, S_{Np}])$ ▷ Evaluate solutions
    $BestTHD_{iter}$=*Min(THD)*
    if *rem(iter,* ρ*)=0&* $BestTHD_{iter} < f(X)$ ***then***
      ▷ *Reset control variables*
      $a = 2, iter_N = 1 and iter_c = 1$
    else ▷ *Reset iter of normalization and chaotic sequence*
      Update$N_{m_{iter}}$, CC_{iter} andCf *by Equation19,20*
      Update$a$, $A$and$C$ *by Equation21,13,12*
    end if
    UpdateX_α, $X_\beta$andX_δ
    $\Delta BestTHD = \frac{\sum_{k=1}^{M}(BestTHD_k - BestTHD_{k-1})}{M}$
    if $\Delta BestTHD < \psi$ **then** ▷ Local Search
      $BestTHD_{iter} = Nelder - Mead(BestTHD_{iter})$
    end if
  end while
  return S, THD ▷ Final solution
end procedure

AGWO is a combination of two processes. First, an adaptive update mechanism tunes **a** based on search performance in the current iteration, which balances exploration and exploitation throughout the search. Second, a chaotic sequence coefficient estimates the normalization function and prevents premature convergence by providing additional benefits.

5 Results and discussion

We evaluate and compare the performance of the proposed optimization method with other meta-heuristics, by using 7-level, 11-level, and 15-level MLIs. To have an accurate comparison, the modulation indexes are tested from 0.3 to 1.5 with an incremental step at 0.1.

5.1 Algorithm comparison in 7-level inverter MLI

The corresponding best-found switching angles and THDs for 7-level inverters using AGWO, mGWO, GWO, PSO, MVO and SSA: are proffered in the Table 1. We used the above meta-heuristics in this work because they have high exploration and exploitation ability to solve real world engineering problems.

From Table 1, the performance of AGWO to optimize THD is higher than that of mGWO, GWO, PSO, MVO and SSA. The average minimum THD proposed by AGWO is 10.43% for a modulation index of 0.84. The near-optimal angles are 8.639°, 27.854°, 49.686° for AGWO for this modulation index. It should be noted that the sum of the results presented in the tables is based on the average of the results of 30 simulations. Moreover, we can note that the application of a static exponential control parameter for mGWO does not perform well in all cases of the modulation indexes compared to standard GWO. Overall, the performance of GWO is more remarkable than that of PSO, MVO, and SSA. The main reason may be the use of a great balance between two search phases: exploration and exploitation.

5.2 Algorithm comparison in 11-level MLI

Optimizing the 11-level MLI problem can be more challenging than the 7-level one because the number of decision variables has increased, leading to a more complex search space. Table 2 presents the obtained average of the best switching angles found for various modulation indexes from 0.3 to 1.0 for 11-level MLI. The best optimization results are suggested by AGWO for all values of the modulation indexes.

Meanwhile, we found that five optimization methods could find the minimum THD values for $M = 0.8$, and also AGWO finds the minimum THD value at 6.09% where the modulation index is 0.81 and the switching angles are $\theta_1 = 5.4253°, \theta_2 = 17.0171°, \theta_3 = 29.1433°, \theta_4 = 42.3308°, \theta_5 = 60.8345°$, respectively. Moreover, the performance of mGWO is considerable as the second best method compared to the original GWO, PSO, MVO and SSA for all values of the modulation indexes. However, it is noted that GWO was able to propose a better switching angle configuration for $M = 0.8$ with 6.174 than mGWO (THD = 6.22, $M = 0.8$). It can be seen that AGWO significantly outperformed both robust optimization methods MVO and SSA considerably and proposed a new switching angle configuration with the minimum THD.

5.3 Algorithm comparison in 15-level MLI

The near-optimal THD and switching angle results for the range of 0.3 and 1.0 modulation indexes in 15-level MLI can be seen in Table 3. Similar to the results of 7-level and 11-level inverters, the mean best THDs and switching angles are explored by AGWO. The best design of the switching angles proposed by AGWO is $\theta_1^\circ = 3.666, \theta_2^\circ = 10.947, \theta_3^\circ = 20.737, \theta_4^\circ = 29.204, \theta_5^\circ = 37.861, \theta_6^\circ = 49.731, \theta_7^\circ = 63.495$, and its THD ($= 0.81$) is 4.30%. Meanwhile, the MVO [27] suggested a lower value of 4.31% for $THD = 0.8$ compared to AGWO and mGWO. Moreover, we can see that the performance of PSO ,and MVO in this system can compete with GWO. Indeed, the adaptive control mechanism for switching between exploration and exploitation leads to a robust and fast search technique. Moreover, the embedded local search assists the AGWO to accurately explore the neighbourhood area of near-optimal configurations. In addition, the experimental results in Table 3 show that both control mechanisms of GWO and mGWO, linear and exponential control models, were not able to avoid the premature convergence.

Figure 6 represents the obtained best switching angles (θ_i) using the proposed adaptive GWO in the modulation index range of 0.3–1.5 with a step size of 0.01 for 7-level (a), 11-level (b), and 15-level (c) inverters. It is observed from Fig. 6, that the switching angles for three systems converge to around zero for modulation indexes larger than one. Second, the optimization process for θ_1 is more difficult than for other switching angles due to a multimodal search space, and also the best angles found for each MLI have decreased in most cases. Last but not least, we can see in Fig. 6 that the near optimal values of the last switching angles such as $\theta_n, \theta_{n-1}, \ldots, \theta_{n/2}$ converge to $\frac{\pi}{2}$ for modulation indexes less than 0.7.

The advantages of the proposed adaptive GWO over other optimizers in this case study are as follows. First and foremost, AGWO is able to converge to an optimum faster than the standard GWO. This is mainly because AGWO adopts an adaptive strategy to switch between the two modes of exploration and exploitation during the optimization process and continuously shrinks the search space. Second, AGWO is equipped with a combined chaotic sequence with the control parameter to avoid local optima. Due to this chaotic tuner, the search capability of AGWO still has a chance to explore even at the end of the optimization process. Last but not least, the adaptive strategy applied in updating the control search parameter in AGWO provides better stability and robustness when the search stagnates and is not able to improve the best

Table 3 Experimental optimization results of adaptive GWO, mGWO, standard GWO, PSO, MVO, and SSA: switching angles, modulation, and THD for 15-level MLI

M	θ_1	θ_2	θ_3	θ_4	θ_5	θ_6	θ_7	THD%
	AGWO							
0.3	7.970	19.983	28.852	43.386	63.151	90.000	90.000	7.020
0.4	5.798	14.443	29.110	35.142	50.698	77.218	90.000	7.260
0.5	0.000	15.394	24.555	32.264	48.570	62.925	89.327	6.590
0.6	5.804	15.473	28.036	41.252	61.113	90.000	90.000	6.250
0.7	5.861	13.231	19.288	26.533	38.561	47.945	60.406	4.820
0.8	4.587	11.895	19.769	30.082	39.175	51.039	65.460	4.330
0.9	0.442	9.902	17.010	30.112	37.179	51.426	63.252	5.790
1	6.138	9.852	21.815	31.392	37.888	50.016	71.921	5.670
	GWO							
0.300	2.086	13.813	35.025	40.723	50.468	79.967	90.000	10.320
0.400	7.499	23.345	38.654	58.545	90.000	90.000	90.000	8.351
0.500	0.201	10.339	18.374	62.142	83.446	90.000	90.000	8.482
0.600	2.912	16.284	28.196	40.633	56.853	90.000	90.000	6.584
0.700	2.614	13.766	23.250	34.109	45.971	61.381	89.395	5.187
0.800	1.689	11.547	20.001	29.054	39.180	51.457	64.268	4.684
0.900	3.671	13.789	19.969	23.640	33.266	48.263	64.747	6.552
1.000	3.336	7.957	19.795	24.397	28.600	44.680	60.701	8.136
	mGWO							
0.300	0.000	14.508	29.731	34.058	53.349	66.366	90.000	8.180
0.400	6.095	22.474	34.535	56.530	90.000	90.000	90.000	8.040
0.500	2.696	16.963	30.134	37.186	55.774	90.000	90.000	7.460
0.600	5.440	16.728	24.091	39.861	48.697	67.176	90.000	6.450
0.700	5.727	13.141	23.669	34.026	45.502	61.650	89.400	5.070
0.800	4.642	11.885	20.177	29.822	39.043	51.263	65.411	4.340
0.900	0.000	9.874	23.819	28.751	39.106	44.256	62.127	6.490
1.000	5.962	4.348	18.356	28.684	33.411	49.992	69.147	7.520
	PSO							
0.300	0.000	24.460	52.210	86.260	90.000	90.000	90.000	15.180
0.400	8.739	24.857	44.737	78.818	89.999	89.999	90.000	11.720
0.500	6.631	19.872	33.617	50.284	84.578	89.999	90.000	8.272
0.600	5.560	15.613	27.473	40.287	54.962	89.001	89.999	6.410
0.700	4.848	13.582	23.750	33.987	46.290	60.898	89.450	5.000
0.800	3.879	11.670	19.489	30.419	38.746	51.193	65.715	4.311
0.900	3.092	9.309	15.615	22.055	28.672	35.541	42.808	12.060
1.000	0.000	2.353	5.464	5.464	7.248	10.727	10.727	42.596
	MVO [27]							
0.400	7.770	25.061	44.763	78.860	90.00	90.00	90.00	11.723
0.500	6.648	19.799	33.534	50.387	84.565	90.00	90.00	8.7256
0.600	5.507	15.619	27.559	40.200	54.926	89.156	89.893	6.418
0.700	4.658	13.630	23.840	33.963	46.316	60.864	89.432	5.00
0.800	3.930	11.534	19.980	30.302	38.874	51.091	65.616	4.311
0.900	3.080	9.264	15.607	22.052	28.612	35.575	42.834	12.060
1.000	0.677	2.129	5.237	5.837	7.103	10.727	10.748	37.316

Table 3 continued

M	θ_1	θ_2	θ_3	θ_4	θ_5	θ_6	θ_7	THD%
	SSA [27]							
0.400	7.663	23.128	45.405	78.967	89.985	89.99	89.99	11.949
0.500	6.739	19.015	33.545	53.664	81.865	89.928	89.947	9.086
0.600	5.923	16.967	27.853	40.422	57.473	86.143	89.955	6.931
0.700	5.109	13.591	23.551	33.859	46.677	61.713	88.348	5.282
0.800	4.969	12.667	20.794	29.779	38.868	50.964	65.290	4.420
0.900	2.415	7.267	12.365	17.404	23.957	32.554	49.177	14.438
1.000	0.00	0.00	0.00	0.00	0.00	0.00	0.00	47.297

found solution compared to PSO, mGWO, GWO, MVO, and SSA.

Figure 7 shows the convergence rate of the AGWO cost function for three MLIs: (a) 7-level, (b) 11-level, and (c) 15-level for modulation indexes ranging from 0.3 to 1. The most important observation can be related to the highest convergence speed in the 7-level MLI. The main reason is that the search space of the 7-level MLI is smoother than the other two systems. Moreover, in three case studies, the minimum cost function is achieved when the modulation index is 0.8 and the lowest convergence rate is considered at $MI = 1$. As a general observation, we can see that there is a direct relationship between the convergence rate and the number of switching angles.

Figure 8 shows the THD values obtained for 7, 11 and 15 MLIs with AGWO for modulation indexes between 0.3 and 1.5. We can notice that the best THD values decreased from 0.3 to 0.8. However, the introduced THD values greater

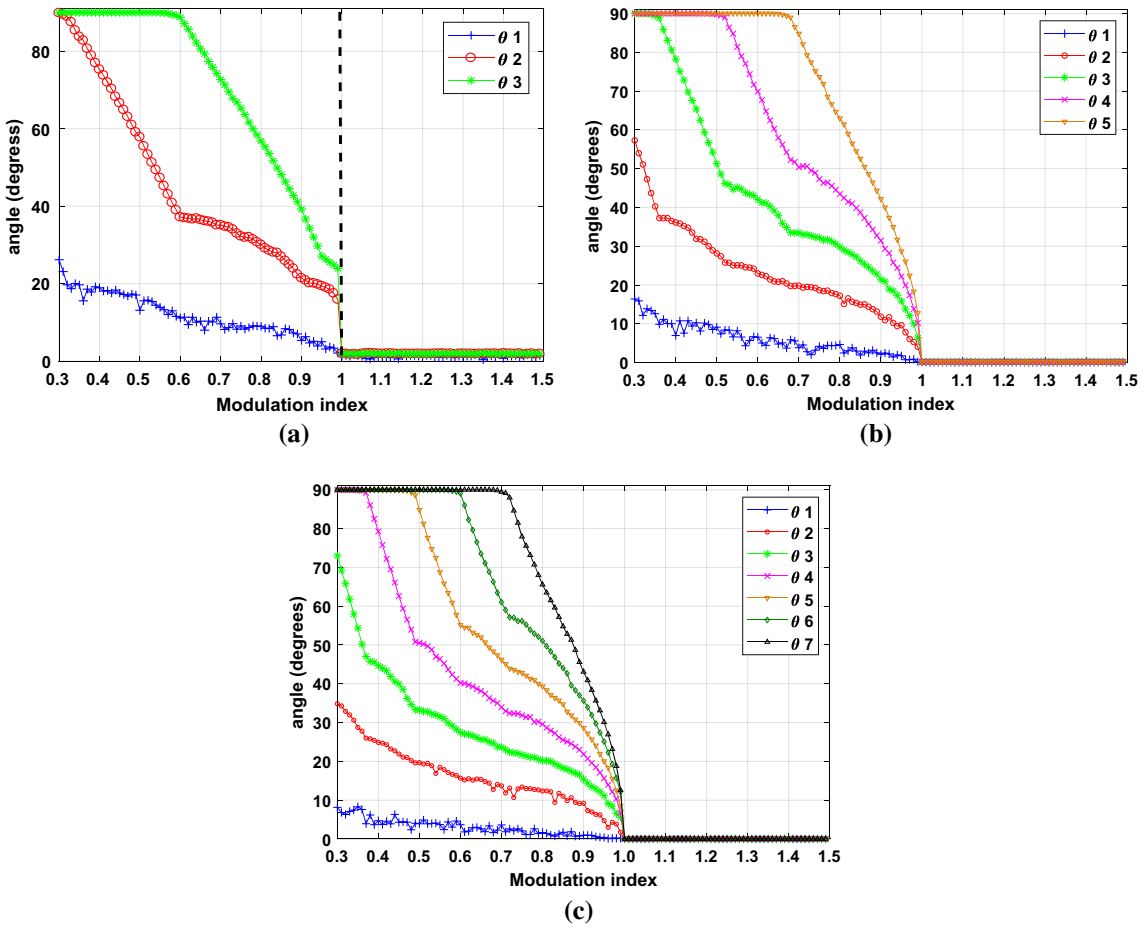

Fig. 6 The average of best-found solutions per each experiment for switching angles and corresponding cost function values for **a** 7-level, **b** 11-level, **c** 15 level cascade MLI

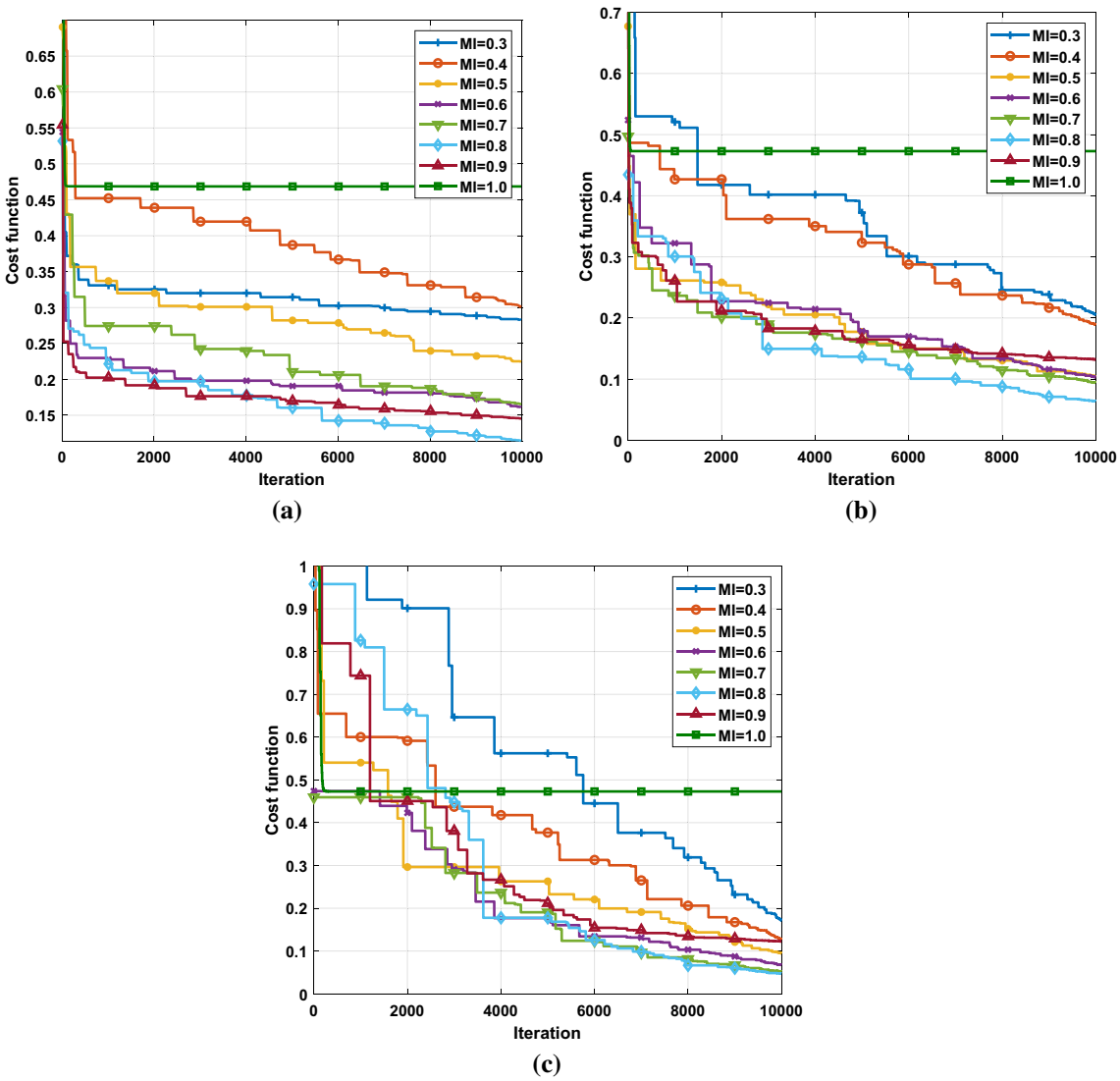

Fig. 7 The convergence speed of AGWO for different values of modulation indexes **a** 7-level, **b** 11-level, **c** 15-level MLIs

than 0.8 to 1.0 have increased. In the following, these values fluctuate with different variances.

6 Conclusion

In this paper, the problem of harmonic elimination and THD minimization was solved utilizing an adaptive GWO with local search capabilities. The simulations were performed with 7-level, 11-level, and 15-level cascaded H-bridge multilevel inverters. Near-optimal switching angles for different modulation indexes were obtained using the proposed algorithms. Moreover, we developed a systematic landscape analysis of cascaded H-bridge multilevel inverters to investigate the characteristics of the search space for this problem. The results of the proposed adaptive GWO were compared with those of the original GWO, mGWO, PSO, MVO, and SSA. It was found that the proposed adaptive GWO is able to solve the optimization problem, which leads to better THD values compared to other meta-heuristics in this study.

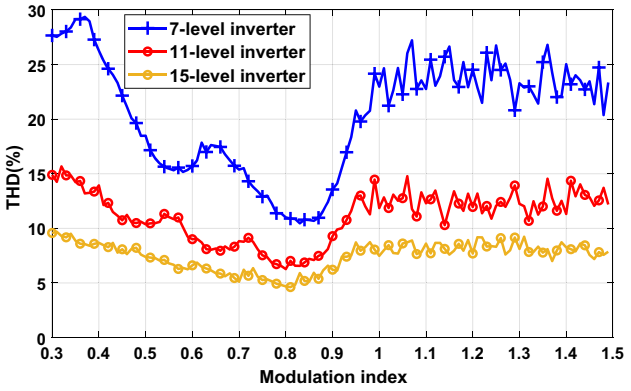

Fig. 8 The average of best-found solutions THD for 7-, 11-, and 15-level MLIs using AGWO

References

1. Ceylan O, Liu G, Tomsovic K (2018) Coordinated distribution network control of tap changer transformers, capacitors and PV inverters. Electr Eng 100(2):1133–1146
2. Wu B, Narimani M (2017) High-power converters and AC drives, 2nd edn. Wiley, Hoboken
3. Poorfakhraei A, Narimani M, Emadi A (2021) A review of multilevel inverter topologies in electric vehicles: current status and future trends. IEEE Open J Power Electron 2:155–170
4. Katir H, Abouloifa A, Noussi K, Lachkar I, Giri F (2022) Cascaded h-bridge inverters for ups applications: adaptive backstepping control and formal stability analysis. IEEE Control Syst Lett 6:145–150
5. Stonier AA, Murugesan S, Samikannu R, Krishnamoorthy V, Subburaj SK, Chinnaraj G, Mani G (2021) Fuzzy logic control for solar PV Fed modular multilevel inverter towards marine water pumping applications. IEEE Access 9:88524–88534
6. Omer P, Kumar J, Surjan BS (2020) A review on reduced switch count multilevel inverter topologies. IEEE Access 8:22281–22302
7. Sunddararaj SP, Srinivasarangan Rangarajan S, Subashini N (2020) An extensive review of multilevel inverters based on their multifaceted structural configuration, triggering methods and applications. Electronics 9(3):433
8. Hossam RM, Hashem GM, Marei MI (2013) Optimized harmonic elimination for cascaded multilevel inverter. In: 2013 48th international universities Power engineering conference (UPEC), pp 1–6
9. Manai L, Armi F, Besbes M (2020) Optimization-based selective harmonic elimination for capacitor voltages balancing in multilevel inverters considering load power factor. Electr Eng 102(3):1493–1511
10. Padmanaban Sanjeevikumar, Dhanamjayulu C, Khan Baseem (2021) Artificial neural network and newton Raphson (ANN-NR) algorithm based selective harmonic elimination in cascaded multilevel inverter for PV applications. IEEE Access 9:75058–75070
11. Son GT, Chung YY, Baek S, Kim HJ, Nam TS, Hur K, Park J (2014) Improved PD-PWM for minimizing harmonics of multilevel converter using gradient optimization. In: 2014 IEEE PES general meeting, conference exposition, pp 1–5
12. Kumar Jagdish, Das Biswarup, Agarwal Pramod (2009) Harmonic reduction technique for a cascade multilevel inverter. Int J Recent Trends Eng 1:181
13. Ozpineci B, Tolbert LM, Chiasson JN (2005) Harmonic optimization of multilevel converters using genetic algorithms. IEEE Power Electron Lett 3(3):92–95
14. Ray RN, Chatterjee D, Goswami SK (2010) A PSO based optimal switching technique for voltage harmonic reduction of multilevel inverter. Expert Syst Appl 37(12):7796–7801
15. Sudha Letha S, Thakur T, Kumar J (2016) Harmonic elimination in a solar powered cascaded multilevel inverter using genetic algorithm and differential evolution optimization techniques. American Society of Mechanical Engineers Digital Collection, New York
16. Majidi B, Baghaee HR, Gharehpetian GB, Milimonfared J, Mirsalim M (2008) Harmonic optimization in multi-level inverters using harmony search algorithm. In: 2008 IEEE 2nd international power and energy conference, pp 646–650
17. Radmanesh H, Kavoosi A (2020) Novel multilevel inverter switching technique based on harmony search algorithm. In: 2020 11th power electronics, drive systems, and technologies conference (PEDSTC), pp 1–6
18. Dahidah MSA, Konstantinou G, Agelidis VG (2015) A review of multilevel selective harmonic elimination PWM: formulations, solving algorithms, implementation and applications. IEEE Trans Power Electron 30(8):4091–4106
19. De Leon-Aldaco SE, Calleja H, Aguayo Alquicira J (2015) Metaheuristic optimization methods applied to power converters: a review. IEEE Trans Power Electron 30(12):6791–6803
20. Memon MA, Siddique MD, Saad M, Mubin M (2021) Asynchronous particle swarm optimization-genetic algorithm (APSO-GA) based selective harmonic elimination in a cascaded h-bridge multilevel inverter. IEEE Trans Ind Electron. https://doi.org/10.1109/TIE.2021.3060645
21. KumarKar P, Priyadarshi A, BhaskarKaranki S (2019) Selective harmonics elimination using whale optimisation algorithm for a single-phase-modified source switched multilevel inverter. IET Power Electron 12(8):1952–1963
22. Mirjalili S, Lewis A (2016) The whale optimization algorithm. Adv Eng Softw 95:51–67
23. Mirjalili S (2015) Moth-flame optimization algorithm: a novel nature-inspired heuristic paradigm. Knowl-Based Syst 89:228–249
24. Ceylan O (2016) Harmonic elimination of multilevel inverters by moth-flame optimization algorithm. In: 2016 international symposium on industrial electronics (INDEL), pp 1–5
25. Mirjalili S, Mirjalili SM, Hatamlou A (2016) Multi-verse optimizer: a nature-inspired algorithm for global optimization. Neural Comput Appl 27(2):495–513
26. Mirjalili S, Gandomi AH, Mirjalili SZ, Saremi S, Faris H, Mirjalili SM (2017) Salp swarm algorithm: a bio-inspired optimizer for engineering design problems. Adv Eng Softw 114:163–191
27. Ceylan O (2020) Multi-verse optimization algorithm-and Salp swarm optimization algorithm-based optimization of multilevel inverters. Neural Comput Appl 33:1935–1950
28. Neshat M, Alexander B, Wagner M (2020) A hybrid cooperative co-evolution algorithm framework for optimising power take off and placements of wave energy converters. Inf Sci 534:218–244
29. Mittal N, Singh U, Sohi BS (2016) Modified grey wolf optimizer for global engineering optimization. Appl Comput Intell Soft Comput. https://doi.org/10.1155/2016/7950348
30. Khomfoi S, Tolbert L (2011) Multilevel power converters. In: Rashid MH (ed) Power electronics handook; devices, circuits and applications, 3rd edn. Butterworth-Heinemann, Oxford, pp 455–487
31. Malan KM, Moser I (2019) Constraint handling guided by landscape analysis in combinatorial and continuous search spaces. Evol Comput 27(2):267–289
32. Mirjalili S, Mirjalili SM, Lewis A (2014) Grey wolf optimizer. Adv Eng Softw 69:46–61
33. Long W, Liang X, Cai S, Jiao J, Zhang W (2017) A modified augmented Lagrangian with improved grey wolf optimization to constrained optimization problems. Neural Comput Appl 28(1):421-438

34. Saxena A, Kumar R, Das S (2019) β-chaotic map enabled grey wolf optimizer. Appl Soft Comput 75:84–105